Interface moving through a random background

Joel Koplik and Herbert Levine
Schlumberger-Doll Research, Old Quarry Road, Ridgefield, Connecticut 06877-4108
(Received 6 February 1985)

We study the motion of a phase interface which is driven through a random background medium, with application to immiscible-fluid displacement in porous media and to random-field Ising systems. The interface motion is described by a local stochastic differential equation, with terms corresponding to an external driving force, interface elasticity, and a random background force. The same equation has been examined by Bruinsma and Aeppli, with whose conclusions we disagree in part. In mean-field theory, we find that the interface can either translate with constant velocity and average width, or be pinned by the random background. The pinning is associated with invasion percolation in the fluid-displacement application and with metastable domains in the Ising case. Perturbation theory in the random term is consistent with the mean-field behavior above three dimensions but diverges in time at lower dimensions, suggesting a transition. The perturbation series appears to be unrenormalizable. By numerical integration of the differential equation, we find that in dimensions less than or equal to 3, the interface pins at sufficiently large randomness but translates essentially as a plane otherwise, while in four dimensions the interface always translates and is never pinned.

I. INTRODUCTION

The motion of a phase boundary in a random medium presents a difficult problem because of its intrinsic nonlinearity and nonlocality. Typically the equation of motion of a boundary point involves interactions both with the medium itself at the point in question, and thus with a random function of the boundary location, and interactions with interior or exterior points through some dynamical field. Direct solutions of such problems[1] are often impractical, and in this paper we consider a *local* approximation to the interface dynamics, in which we hypothesize an evolution equation for a point on the phase boundary. We are encouraged to do so by recent work on dendritic growth,[2] where local approximations to an analogous heat-diffusion problem have led to very promising results. Even after this approximation, we still face severe nonlinearities due to the randomness, and the resulting analysis is still quite complicated.

We shall illustrate the general aspects of the problem and the nature of the local approximation using the example of immiscible-fluid displacement in porous media,[3] as occurs during the flow of oil and water in hydrocarbon reservoirs. The situation is shown schematically in Fig. 1 in two dimensions, where water is forced by a pressure gradient into an oil-filled porous medium (e.g., sandstone rock). Each fluid satisfies a Navier-Stokes equation with boundary conditions of zero velocity ("no-slip") on the pore space boundary, and at the oil-water interface the velocity is continuous and surface tension exerts a normal stress. The system is nonlocal because the velocity on the fluid is determined by the global solution of the Navier-Stokes equation, and is effectively nonlinear (even at low velocities when the equation can be linearized) because each fluid's concentration satisfies a nonlinear equation of continuity. Randomness enters both in the no-slip condition on the irregular solid boundary, and through the fact that the surface-tension force, proportional to the local curvature of the oil-water menisci, varies both in magnitude and direction as the fluids move about (see the blow-

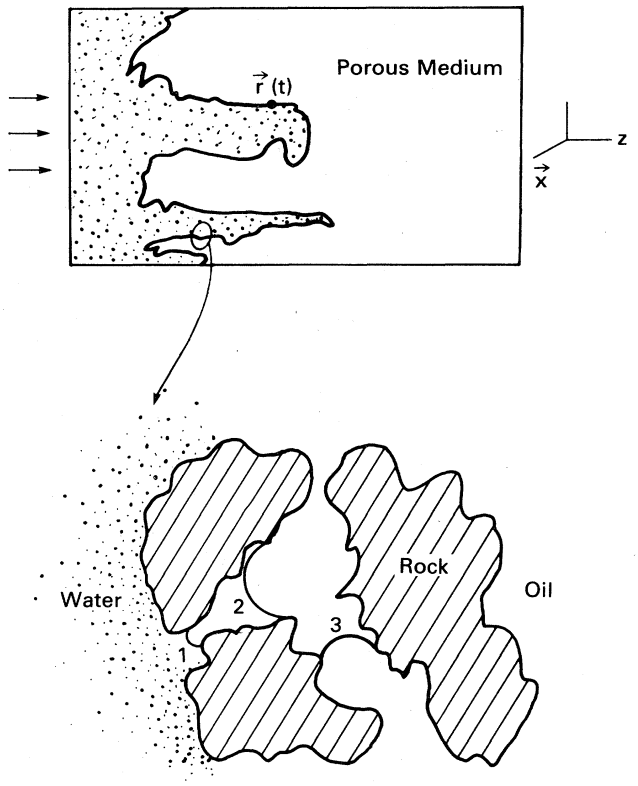

FIG. 1. Illustration of a fluid-fluid interface in a porous medium at the macroscopic and microscopic length scales.

up in Fig. 1). These complications are so severe that even numerical computations in simplified geometries[4] are quite time consuming and not sufficiently informative. Typically one is really interested in the average or large-scale behavior of the interface, but even this cannot be found without first obtaining the microscopic solution.

As in our earlier work on dendritic growth,[2] we construct a simplified local model of this process by writing the velocity of a point on the interface as a sum of terms representing different physical mechanisms acting on it. Considering the interface at the "macroscopic" scale of many rock grains (as in the upper part of Fig. 1), if $\mathbf{r}(t)$ is a point on the oil-water interface at time t, in d spatial dimensions, we write its normal velocity as

$$\hat{\mathbf{n}}\cdot\frac{d\mathbf{r}(t)}{dt}=v_0(\mathbf{r})-J\kappa+g\eta(\mathbf{r}) . \tag{1}$$

In this equation, κ and $\hat{\mathbf{n}}$ are the mean curvature and normal to the interface at $\mathbf{r}$, and the origin of the various terms is as follows. In the absence of randomness in the porous medium, a pressure gradient would displace a fluid boundary with some macroscopic average normal velocity, v_0. The second term approximately represents the effects of viscosity: if the interface develops a long narrow finger, as in Fig. 1, the finger will slow down because of the difficulty in moving viscous fluid through a narrow channel. The term "long, narrow finger" is of course an intrinsically nonlocal concept, but to have a tractable equation we make the simple approximation of slowing regions of high curvature. The effect of viscosity is actually somewhat subtle, since it is known[3] that in porous media a macroscopic displacement front is smooth (e.g., planar or circular) when the "mobility" of the displacing fluid is less than that of the displaced fluid, and develops fingers otherwise. Now the mobility is inversely proportional to the velocity, so viscosity is potentially destabilizing, but the macroscopic behavior results from a combination of the physical properties and spatial arrangements of the fluids as well as the randomness of the porous medium. We will study the case of mobility *stabilization,* where our ansatz is certainly appropriate; further discussion of this point is given in the conclusions.

The last term in (1) represents the random capillary forces exerted by surface tension. g is the strength and η is a random variable with zero mean (the average capillary force is included in v_0) and δ-function correlation

$$\langle\eta(\mathbf{r})\rangle=0, \quad \langle\eta(\mathbf{r})\eta(\mathbf{0})\rangle=\delta^d(\mathbf{r}) . \tag{2}$$

Figure 1 suggests that in fact the capillary force will be correlated over a distance of order a grain diameter, but Eq. 1 is meant to apply on much larger scales. In practice we shall regularize the δ function to have well-defined integrals, and to avoid subtleties of Ito and Stratonovich integration.[5] We do not write an equation for the tangential velocity, because tangential motion just relabels points on the interface. A stochastic differential equation is equivalent to a quantum-field theory, and so the parameters v, J, and g should be thought of as bare quantities in the sense that the nonlinearity of the equation will mix all three effects and, for example, the actual velocity of the interface will be some function of all three.

We make one further simplification, corresponding to a solid-on-solid approximation,[6] and formally assume that the interface is nearly flat and can be specified as $z=f(\mathbf{x},t)$, where $\mathbf{x}$ is a $(d-1)$-dimensional transverse coordinate, and where $|\nabla f|\ll 1$. The stochastic differential equation then simplifies to

$$\frac{\partial f}{\partial t}=v+J\nabla^2 f+g\eta(\mathbf{x},f) . \tag{3}$$

Note that η is still a function of d coordinates, and is evaluated at the position of the interface. We have taken the "bare" normal velocity to be a constant, corresponding to the macroscopic quasi-one-dimensional geometry of Fig. 1. Equation (3) has most of the qualitative features used to motivate (1), except for reparametrization and rotational invariance, and could just as well have been taken as the starting point. One important difference is that a general interface may intersect itself, corresponding to the formation of domains of one fluid trapped in another. However, this effect is intrinsically nonlocal, and cannot be addressed within the context of a local model. Some further discussion of this point appears in Sec. VI.

We are interested in the time dependence of the interface, averaged over different regions of the random medium, which we can compute by averaging over different realizations of the random variable η. The objects of interest are such quantities as $\langle f(t)\rangle$ and $\langle[f(t)-\langle f(t)\rangle]^2\rangle$, the average displacement and width of the interface. These quantities are independent of $\mathbf{x}$ because of the translation invariance of (1) and (2). The average displacement gives the speed of the process when it is increasing with time, and indicates the presence of an "invasion-percolation" regime[7] when it becomes time independent. The latter case refers to a situation occurring when the injection of water is so slow that the motion reduces to a succession of slow meniscus jumps through points of "least resistance" or greatest instability. In the invasion-percolation regime, the interface advances as a fractal and occupies a volume of dimension less than d, giving no contribution to $\langle f\rangle$. This phenomenon might be expected when g/v, suitably nondimensionalized, is large and will be referred to in general as "interface pinning." The interface width is of interest because it gives the size of the largest blobs of oil that can be surrounded by water and trapped by capillary forces,[8] and higher moments of f could be used to infer the distribution of interface fluctuations and thence of trapped blob sizes.

Our model equation (3) has been introduced independently by Bruinsma and Aeppli[9] to study the motion of domains in the random-field Ising model. They argued that the position $f(\mathbf{x},t)$ of the interface between spin-up and spin-down domains could be thought of as an order parameter in the Landau-Ginsburg sense, and in a time-dependent situation would satisfy the relaxational equation

$$\frac{\partial f}{\partial t}=v-\frac{\delta F}{\delta f} , \tag{4}$$

where v represented either an external magnetic field or a chemical potential difference between phases, and where F is the random Ising free energy introduced by Grinstein

and Ma,[10]

$$F[f]=\int d^{d-1}x\left[\tfrac{1}{2}J\,|\,\nabla f\,|^2-\int_{-\infty}^{f(\mathbf{x},t)}dz\,g\eta(\mathbf{x},z)\right]. \tag{5}$$

The first term represents a familiar membrane elastic energy, while the second is the energy difference between the up and down spin domains, η being the local random magnetic field and g its coupling to a spin. Equations (4) and (5) combine to reproduce (3). In this problem, one is interested in the persistence or decay of a domain of one spin surrounded by an ordered phase of the other, and whether the boundary of an energetically unfavored domain may be pinned by sufficiently large randomness, corresponding to a long-lived metastable state.

The motivating arguments of Bruinsma and Aeppli could equally well have been used for the fluid-displacement problem, and conversely, our motivating arguments for (3) could have been used for the magnetic problem. Presumably, other physical problems in random media could be formulated as the same or a similar stochastic differential equation. Although the equation is heuristic in origin, particularly in regards to the terms in v and J, the random term seems to us a very natural way to model the effect of a stochastic background on a moving interface. As we shall see, the severe nonlinearity introduced by the randomness is the essential difficulty of the problem, and it does not appear worthwhile in the present context to attempt to improve the realism of the other terms.

One might wonder why we have not included an additional random term corresponding to thermal fluctuations. In the fluid flow case, the interface corresponds to a set of capillary menisci which are large on the atomic scale (typically of radius 0.1—10 μm), and thermal noise is negligible. For the Ising case, it has been shown[10] that the random-field effects dominate any possible pinning transition, although thermal fluctuations will control the subsequent relaxation of metastable states to equilibrium.

The remainder of this paper describes our (only partially successful) attempts to solve (3). In Sec. II we discuss some elementary properties, in various simple limits, and also review the scaling arguments of Bruinsma and Aeppli. In Secs. III—V we attempt to analyze the equation using the standard sequence: mean-field theory → perturbation theory → renormalized perturbation theory. In this problem mean-field theory consists of replacing the continuum by a transverse lattice, replacing the interface at neighboring points by a to-be-determined mean-field value, and solving self-consistently and order by order in g for the latter. Mean-field solutions can be either pinned or uniformly translating. In straightforward perturbation theory in g, we find that the translating solutions are consistent in dimensions $d>3$, but the series diverges in time otherwise, with terms of the form $g^{2n}(t/a)^{n(3-d)/2}$, where a is a short-distance cutoff. We are then led to attempt to use the renormalization group to sum the series near $d=3$, but we find divergences that cannot be absorbed into the bare parameters. In Sec. VI we discuss the numerical integration of the equation. We find that for $d\leq 3$, the interface will become pinned for sufficiently large randomness, but never pins in $d=4$. This behavior is consistent with perturbation theory and with results of Villain[11] (obtained through different arguments), but disagrees with the scaling argument of Bruinsma and Aeppli which predicts a transition at $d=5$. Other aspects of the behavior of the interface are found to be weak functions of the coupling J, also in disagreement with the scaling results.[9] Some concluding remarks are given in Sec. VII.

II. PRELIMINARY ARGUMENTS

Before embarking on a detailed analysis, we wish to discuss some elementary properties of the basic equation (3). First, it will often be convenient to rewrite it as the nonlinear integral equation

$$f(\mathbf{x},t)=vt+g\int d^{d-1}x'\int_0^t dt'G(\mathbf{x}-\mathbf{x}',t-t')\eta(\mathbf{x}',f,(\mathbf{x}',t'))+\int d^{d-1}x'\,G(\mathbf{x}-\mathbf{x}',t)f(\mathbf{x}',0) \tag{6}$$

in terms of the diffusion Green's function

$$G(\mathbf{x},t)=\frac{1}{(4\pi Jt)^{(d-1)/2}}\exp\left[\frac{-\mathbf{x}^2}{4Jt}\right]. \tag{7}$$

In the absence of the random term η, any initial interface profile $f(\mathbf{x},0)$ would "diffuse away" transversely, and the asymptotic shape would be a translating plane, $f=vt$. In the subsequent arguments, we will assume the initial shape is $f=0$.

A more interesting simplification is obtained by replacing $f(\mathbf{x}',t')$ in the argument of η in the second term of (6) by vt', on the grounds, say, that both of these quantities will cause a fluctuation in the value of η as the interface moves. (This approximation resembles the "kinetic drumhead model" studied by Kawasaki and Ohta,[12] which differs by having a polynomial nonlinearity in f instead of a drift term.) In this case (6) can be solved immediately, to give $\langle f\rangle=vt$ and interface width

$$\langle(f-vt)^2\rangle=g^2\int d\mathbf{x}_1\int d\mathbf{x}_2\int_0^t dt_1dt_2G(\mathbf{x}-\mathbf{x}_1,t-t_1)G(\mathbf{x}-\mathbf{x}_2,t-t_2)\langle\eta(vt_1,\mathbf{x}_1)\eta(vt_2,\mathbf{x}_2)\rangle\,.$$

This integral is singular with the δ-function correlation (2), so we regularize it using a short-distance cutoff a,

$$\langle \eta(\mathbf{x},z)\eta(\mathbf{0},0)\rangle = \frac{1}{(\pi a^2)^{d/2}} e^{-(\mathbf{x}^2+z^2)/a^2} \tag{8}$$

which leads to

$$\langle (f-vt)^2\rangle = \frac{g^2}{(\pi a^2)^{1/2}} \int_0^t dt_1 dt_2 [a^2+4J(2t-t_1-t_2)]^{-(d-1)/2} e^{-[v(t_1-t_2)/a]^2}$$

$$\underset{t\to\infty}{\sim} \frac{g^2}{Jv} \begin{cases} (Jt)^{(3-d)/2}, & d<3 \\ \ln\left[\dfrac{Jt}{a^2}\right], & d=3 \\ a^{3-d}, & d>3 . \end{cases} \tag{9}$$

For a fixed random background medium, this simplified model is probably an *oversimplification,* because it throws out the fact that the random background medium is fixed. For example, if the interface at transverse coordinate $\mathbf{x}$ arrives at a point where the random term is large and negative, it should tend to hold up or reverse direction, but under the simplified equation the random term will fluctuate at the next instant and this part of the interface can be freed. The simplified model is analogous to the Eden model[13] of cluster growth where particles accrete randomly in time, whereas (3) or (6) corresponds to diffusion-limited aggregation[14] where accretion is influenced by the present and previous cluster shape. In a loose sense, the simplified model is a lower bound on the irregularity of the interface. An upper bound, again loosely speaking, is obtained by replacing the random term by $\eta(\mathbf{x},0)$, corresponding to grooves whose size is a random function of transverse coordinate and which extend indefinitely in the longitudinal direction. In this case one finds a result similar to (9) but with $(3-d)$ replaced by $(5-d)$, enhancing the interface width as expected.

Although the basic equation cannot be solved in closed form even in zero transverse dimensions, where

$$\frac{\partial f(t)}{\partial t} = v + g\eta(f(t)) , \tag{10}$$

the qualitative character of the solution is easily found. Suppose $v>0$ for definiteness, and that the random term has been regularized. When v is larger than the product of g and the maximum value of η, $\partial f/\partial t$ is always positive and the interface always moves, with an instantaneous velocity fluctuating about v. When v is less than the above value, the interface eventually arrives at a point where $v+g\eta=0$, and stops. Thus for fixed v, as g increases from zero a pinning transition occurs at some finite value. [Equations similar to (10) have been studied by several authors in the context of diffusion in a random medium.[15] In this problem one explicitly includes time-dependent random terms corresponding to thermal fluctuations, and in consequence the behavior is subdiffusive rather than pinned.]

In the opposite limit of very large transverse dimensionality, Bruinsma and Aeppli[9] argue that pinning will never occur. Suppose the transverse coordinates are discretized on a lattice of N sites per direction. The Laplacian term in (3) tends to make $f(\mathbf{x},t)$ equal to the average of f at neighboring points, and as $d\to\infty$ there will be an infinite number of neighbors, and this term will force the interface to be flat. Summing (3) over all transverse coordinates then yields

$$\frac{\partial}{\partial t}\sum_{\mathbf{x}} f(\mathbf{x},t) = vN^{d-1} + 0 + O(gN^{(d-1)/2}) > 0 \tag{11}$$

using the fact that the typical fluctuation in the sum of n independent random variables is $O(n^{1/2})$.

These arguments suggest that a pinning transition occurs at finite g in low dimension but disappears for sufficiently large d. Bruinsma and Aeppli attempted to identify the transition dimension using a scaling argument. If the interface position is taken as dimensionless and the transverse coordinates have a lattice spacing a, (3) can be written

$$\frac{\partial f(\mathbf{x}_k,t)}{\partial t} = v + \frac{J}{a^2}\sum_{i=-(d-1)}^{d-1} D_i D_i f + \frac{g}{a^{(d-1)/2}}\epsilon(\mathbf{x}_k,f) , \tag{12}$$

where D_i is a finite difference operator and ϵ has Kronecker delta correlation in $\mathbf{x}$. From the structure of (12), the "depinning force," the value of v at which the interface will become pinned, must be of the form

$$v_c = \frac{g}{a^{(d-1)/2}}\phi\left[\frac{J}{g}a^{(d-5)/2}\right] \tag{13}$$

by dimensional analysis. Similarly, the "width of the interface on a length scale L" (Ref. 9) has the form $W_L \sim (g/J)L^{(5-d)/2}$. Thus for $d>5$, W_L vanishes as $L\to\infty$, the interface is flat, and from (11), $v_c=0$. For $d<5$, $W_L \lesssim 1$ for $L<L_0\sim(g/J)^{2/(d-5)}$, so one can preaverage over length scales less than L_0, in effect replacing a by L_0 in v_c, obtaining

$$v_c \sim g\left[\frac{g}{J}\right]^{(d-1)/(5-d)} , \quad d<5 . \tag{14}$$

This is a somewhat heuristic argument, and even an ambiguous one, since if one chooses to regard all d coordinates as dimensionful, these steps can be repeated with the transition now occurring for $d=2$ and with $(5-d)\to(2-d)$. The subsequent results in this paper disagree with these detailed scaling arguments, although

they do support the qualitative picture of a transition.

III. MEAN-FIELD THEORY

The first step in systematically analyzing the model is to construct the mean-field theory. To do this,[16] we consider the transverse coordinates as lying on a lattice of spacing a and rewrite the Laplacian term in (3) as

$$J\nabla^2 f(\mathbf{x},t)\to\frac{J}{a^2}\sum_{i=-(d-1)}^{d-1}[f(\mathbf{x}+\hat{e}_i,t)-f(\mathbf{x},t)]$$
$$\to\frac{(d-1)J}{a^2}[\phi(t)-f(\mathbf{x},t)]\ ,$$

where $\phi(t)$ is the mean field, to be determined by the self-consistency requirement

$$\langle f(\mathbf{x},t)\rangle=\phi(t)\ . \tag{15}$$

The interface equation is now independent of transverse coordinate,

$$\frac{\partial f(t)}{\partial t}=v+\tilde{J}[\phi(t)-f(t)]+g\eta(f(t))\ , \tag{16}$$

where $\tilde{J}=J(d-1)/a^2$. We can solve (15) by a power series in the random interaction, writing

$$f(t)=\sum_{n=0}^{\infty}g^n f_n(t),\quad \phi(t)=\sum_{n=0}^{\infty}g^n\phi_n(t) \tag{17}$$

and identifying powers of g. First we consider $v\neq 0$. In lowest order we have

$$\dot{f}_0=v+\tilde{J}(\phi_0-f_0)\ ,$$

from which $\langle\dot{f}_0\rangle=v$, and $\langle f_0\rangle=vt=\phi_0$. At next order,

$$\dot{f}_1=\tilde{J}(\phi_1-f_1)+\eta(vt)$$

so that $\langle\dot{f}_1\rangle=0$, and $\langle f_1\rangle=\phi_1=$ const, which can be set to zero, and

$$f_1(t)=e^{-\tilde{J}t}\int_0^t dt' e^{\tilde{J}t'}\eta(vt')\ .$$

The first nontrivial order is

$$\dot{f}_2=\tilde{J}(\phi_2-f_2)+\eta'(vt)f_1(vt)\ .$$

Taking the average, and using the previous expression for f_1, we find

$$\dot{\phi}_2=\frac{-1}{2a^2}\frac{1-e^{-(\tilde{J}+v/a)t}}{\tilde{J}+v/a}$$

where we have used the convenient regularization

$$\langle\eta(z)\eta(0)\rangle\equiv C(z)=\frac{1}{2a}e^{-|z|/a}\ . \tag{18}$$

Taking the limits $t\to\infty$ and then $a\to 0$, we have $\phi_2\to -t/2av$. The solution for f_2 is then

$$f_2(t)=e^{-\tilde{J}t}\int_0^t dt'\left[\tilde{J}e^{\tilde{J}t'}\phi_2(t')+\eta'(vt')\int_0^{t'}dt''e^{\tilde{J}t''}(vt'')\right]\ .$$

At the next order, because f_3 involves three factors of η, $\langle\dot{f}_3\rangle=0$, so $\langle f_3\rangle=\phi_3=0$, and

$$f_3(t)=e^{-\tilde{J}t}\int_0^t dt' e^{\tilde{J}t'}[\tfrac{1}{2}\eta''(vt')f_1^2(t')+\eta'(t')f_2(t')]\ .$$

In fourth order,

$$\dot{f}_4=\tilde{J}(\phi_4-f_4)+\frac{1}{3!}\eta''(vt)f_1^3+\eta''(vt)f_1f_2+\eta'(vt)f_3\ .$$

When this expression is averaged, the terms independent of ϕ_2 tend to constants as $t\to\infty$, because the lower order f's always enter in the combination

$$e^{-\tilde{J}t}\int_0^t dt' e^{\tilde{J}t'}\eta\cdots\ .$$

The other two terms cancel due to the identity $\langle\eta''\eta+\eta'\eta'\rangle=0$.

In higher orders, the general structure of terms is that f_n involves n η's, and

$$\dot{f}_n=\tilde{J}(\phi_n-f_n)+\sum_{i=1}^{n-1}\eta^{(i)}(vt)\sum_{\mathbf{j},\mathbf{k}}c(\mathbf{j},\mathbf{k})f_{j1}^{k1},\ldots,f_{j_i}^{k_i}\ ,$$

where $j_i,k_i\geq 1$, $\sum k_i\leq i$, and $\sum j_i k_i=n-1$. Thus $\langle\dot{f}_{2n+1}\rangle=0$ which implies $\phi_{2n+1}=0$, while $\langle\dot{f}_{2n}\rangle\to$ constant as $t\to\infty$ by the same reasoning as for f_4. The latter argument could be invalidated by the appearance of terms involving lower order ϕ_{2n}'s, which could produce positive powers of t, but at least through order g^6 where we have had the patience to check, they cancel.

The interface width is calculable once the f_n are known. To lowest nonvanishing order,

$$\langle[f-\phi]^2\rangle=g^2\langle f_1^2\rangle\to\frac{g^2}{2v\tilde{J}}\quad\text{as } t\to\infty\ .$$

To next order, g^4, the relevant terms are $\langle f_2^2+2f_1f_3\rangle-\langle f_2\rangle^2$, and after some straightforward algebra are seen to approach constants as $t\to\infty$. Therefore, for any $v\neq 0$, $\tilde{J}$, and g, there exists a mean-field solution which asymptotically propagates with constant velocity and width. Note that the averages diverge order by order in g as $a\to 0$, reflecting the highly singular nature of the governing equation. In summary, there is a propagating mean-field interface with velocity and width given by

$$\phi(t)=vt\left[1-\frac{g^2}{2av^2}+\sum_{n=1}^{\infty}\left[\frac{g^2}{av^2}\right]^n U_n\left[\frac{\tilde{J}a}{v}\right]\right]\ , \tag{19a}$$

$$\langle[f(t)-\phi(t)]^2\rangle=\frac{g^2}{2v\tilde{J}^2}\left[1+\sum_{n=1}^{\infty}\left[\frac{g^2}{av^2}\right]^n V_n\left[\frac{\tilde{J}a}{v}\right]\right]\ . \tag{19b}$$

In view of the relevance of pinned solutions, one may also look for power-series solutions of (16) for $v=0$. At order g^0, $\dot{f}_0=\tilde{J}(\phi_0-f_0)$, so $f_0=\phi_0=0$. At next order,

$$\dot{f}_1=\tilde{J}(\phi_1-f_1)+\eta(0)$$

with solution $\phi_1=0$ and

$$f_1=\frac{1}{\tilde{J}}\eta(0)(1-e^{-\tilde{J}t})\ .$$

In the last two formulas, $\eta(0)$ should be interpreted as an inverse cutoff. In the same spirit, $\eta'(0)=0$, so that at

second order

$$\dot{f}_2=\tilde{J}(\phi_2-f_2)+\eta'(0)f_1 \ .$$

The second term on the right does not contribute, and $\dot{\phi}_2=\phi_2=f_2=0$. The calculation proceeds in this way in higher orders: for odd n an odd number of η's appear on the right and on averaging one finds $\dot{\phi}_n=0=\phi_n$, while for even n at least one $\eta(0)$ is differentiated an odd number of times and the result is the same. The interface width may be calculated as before; to lowest order it is $\langle f_1\rangle^2=g^2/2a\tilde{J}^2$, and is similarly seen to remain constant in higher orders in g. Therefore we also have stationary mean-field solutions with width

$$\langle[f(t)-\phi(t)]^2\rangle=\frac{g^2}{2a\tilde{J}^2}\left[1+\sum_{n=1}^{\infty}W_n\left[\frac{g^2}{\tilde{J}^2a^3}\right]^n\right] . \tag{20}$$

As usual, a calculation beyond mean-field theory is needed to decide which if any of the mean-field solutions is relevant.

IV. PERTURBATION THEORY

We now turn to the solution of the stochastic interface model by perturbation series in g; this calculation is similar to that used in mean-field theory but has the additional complication that the individual terms also involve an integration over transverse variables. The expansion is formally about a plane interface propagating with the bare velocity v, which is not at all guaranteed to be a close enough approximation to the actual solution to be a suitable starting point. (For example, the appearance of inverse powers of v in (19) suggests an essential singularity at $v=0$.) However, we have been unable to find another analytic method which produces an intelligible result and does not break down or lead to inconsistencies, so we shall proceed with what is available.

We consider the integral equation form of Eq. (6) with the last term dropped by taking the initial interface to be the plane $f=0$. To keep track of the various terms, it is convenient to use a diagrammatic expansion. We expand the interface position in powers of g as

$$f(\mathbf{x},t)=\sum_n g^n f^{(n)}(\mathbf{x},t) \ ,$$

and collect powers of g. Schematically denoting a space-time point by an integer, $1\equiv(\mathbf{x}_1,t_1)$, etc., and integration over space and time by a repeated integer, e.g.,

$$G_{12}f_2\equiv\int d\mathbf{x}_2\int_0^{t_1}dt_2G(\mathbf{x}_1-\mathbf{x}_2,t_2-t_1)f(\mathbf{x}_2,t_2) \ ,$$

the expansion is

$$\begin{aligned} f_1^{(0)}&=vt \ , \\ f_1^{(1)}&=G_{12}\eta_2 \ , \\ f_1^{(2)}&=G_{12}\eta_2'G_{23}\eta_3 \ , \\ f_1^{(3)}&=G_{12}(\eta_2'G_{23}\eta_3'G_{34}\eta_4+\tfrac{1}{2}\eta_2''G_{23}\eta_3G_{24}\eta_4) \ , \end{aligned} \tag{21}$$

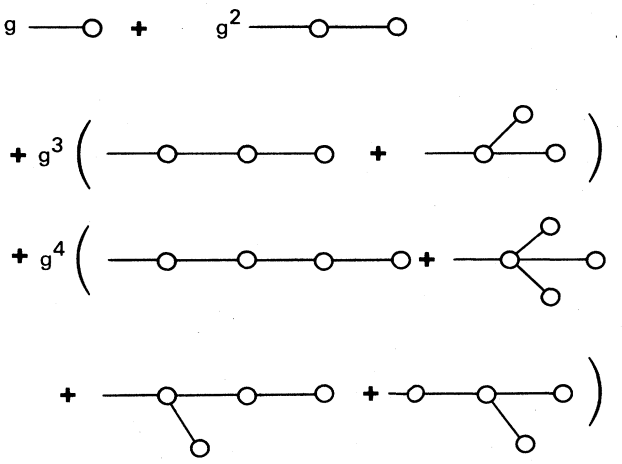

FIG. 2. Schematic form of the perturbation expansion (21).

and so on. The expansion is shown pictorially in Fig. 2; a solid line corresponds to a G and a vertex to an $\eta^{(k)}$, where the superscript means a differentiation k times with respect to the argument vt, k being the number of lines leaving the vertex to the right. The vertices are ordered, with time increasing from right to left, and their space and time positions are integrated over. The nth-order generalization of (21) corresponds to all tree graphs with n vertices. The calculation of Gaussian averages $\langle\ \rangle$ consists of pairing the η's in all possible ways and inserting the correlation function (9), and graphically involves connecting the vertices pairwise, as illustrated in Fig. 3.

We begin with the $O(g^2)$ terms. The interface width has in fact been computed in Sec. II to this order, with the result shown in (9). The interface position is given by the similar expression, associated with the diagram in Fig. 3(a),

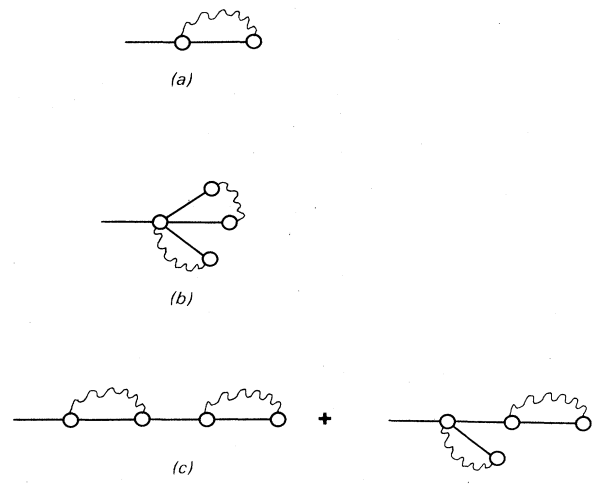

FIG. 3. Examples of contractions corresponding to terms in the perturbation series.

$$\langle f^{(2)}(\mathbf{x},t)\rangle = \int d\mathbf{x}_1 \int d\mathbf{x}_2 \int_0^t dt_1 \int_0^{t_1} dt_2 G(\mathbf{x}-\mathbf{x}_1)G(\mathbf{x}_1-\mathbf{x}_2)\langle \eta'(vt_1,\mathbf{x}_1)\eta(t_2,\mathbf{x}_2)\rangle \ .$$

We insert (7) for the G's and (8) for the correlation function, and integrate over the $\mathbf{x}_i$ to find

$$\langle f^{(2)}\rangle = \int_0^t dt_1 \int_0^{t_1} dt_2 (a^2+t_1-t_2)^{-(d-1)/2} \frac{\partial}{\partial(vt_1)} \frac{1}{\pi^{1/2}a} e^{-[v(t_1-t_2)/a]^2} \ .$$

The exponential forces $t_2 = t_1 + O(a)$, so the t_2 integral is a constant, leaving $\sim \int_0^t dt_1 \sim t$. Explicitly, with non-numerical constants restored,

$$\langle f^{(2)}\rangle \sim -\frac{g^2}{av}\left[\frac{v}{aJ}\right]^{(d-1)/2} t \quad \text{as } t\to\infty \tag{22}$$

which is a negative correction to the velocity.

At order g^4, we contract the relevant diagrams of Fig. 3, giving nine distinct terms. We illustrate the calculation with the contraction shown in Fig. 3(b),

$$\langle f^{(4)}(\mathbf{x},t)\rangle_{3(b)} = \tfrac{1}{2}\int d\mathbf{x}_1 \int d\mathbf{x}_2 \int d\mathbf{x}_3 \int d\mathbf{x}_4 \int_0^t dt_1 \int_0^{t_1} dt_2 dt_3 dt_4 G(\mathbf{x}_{01},t_{01})G(\mathbf{x}_{12},t_{12}) \ ,$$
$$\times G(\mathbf{x}_{13},t_{13})G(\mathbf{x}_{14},t_{14})C'''(\mathbf{x}_{12},vt_{12})C(\mathbf{x}_{34},vt_{34}) \ ,$$

where $t_{ij}=t_i-t_j$, similarly for $\mathbf{x}_{ij}$, and C is differentiated with respect to its second argument. Using Eqs. (7) and (8) and integrating over the $\mathbf{x}_i$, this becomes

$$\langle f^{(4)}(\mathbf{x},t)\rangle_{3(b)} = \tfrac{1}{2}\int_0^t dt_1 \int_0^{t_1} dt_2 \int_0^{t_1} dt_3 \int_0^{t_1} dt_4 [(a^2+t_{12})(a^2+t_{13}+t_{34})]^{-(d-1)/2}$$
$$\times \left[\frac{12vt_{12}}{a^4} - \frac{8(vt_{12})^3}{a^6}\right] e^{-(vt_{12})^2/a^2} \frac{1}{\pi^{1/2}a} e^{-(vt_{34})^2/a^2} \ .$$

For the t_4 integral, we may take $a\to 0$ in the last two factors and simply set $t_3=t_4$. Suppose for the moment that $d<3$; the t_3 integral is then

$$\int_0^{t_1} dt_3 (a^2+t_{13})^{-(d-1)/2} \sim t_1^{(3-d)/2} \quad \text{as } t_1\to\infty \ .$$

The remaining integrals are

$$\sim \int_0^t dt_1 t_1^{(3-d)/2} \int_0^{t_1} dt_{12} h(t_{12}) \sim t^{(5-d)/2}$$

because the function h is sharply peaked about zero and the second integral is a t_1-independent constant. Similarly, for $d=3$ the t_3 integral is proportional to $\ln t_1$ and the remaining integrals give $\sim t\ln t$, and for $d>3$ the t_3 integral is constant and the result $\sim t$. The remaining contractions are analyzed in the same way, and lead to terms of the same or subdominant t dependence. There are individual diagrams that behave as t^2, shown in Fig. 3(c), but their leading behavior cancels. The net result through fourth order, restoring the dimensional constants, is

$$\langle f(\mathbf{x},t)\rangle = vt\{1 - g^2 c_2 J^{(1-d)/2} a^{-(3+d)/2} v^{(d-5)/2} + g^4[c_4 J^{(1-d)/2} a^{-(d+5)/2} v^{(d-7)/2} t^{(3-d)/2} + O(t^0)] + O(g^6)\} \ , \tag{23}$$

where $c_{2,4}$ are numbers. The result is written for $d<3$; for $d=3$, $t^{(3-d)/2}$ is replaced by $\ln(Jt/a^2)$, and for $d>3$ it is replaced by $a^{(3-d)/2}$. In the next order there are too many diagrams for us to compute; there are individual terms which behave as t^3 and t^2, which cancel, and the survivors seem to be $\sim (t^{(3-d)/2})^2$.

The series solution (23), and its counterpart for the width (9), suggest a transition at $d=3$. For higher dimensions, the corrections to a plane, uniformly propagating interface are t independent, and we have a consistent solution of the equation. At $d\le 3$ however, this is not the case, and one may suspect a different behavior. Unfortunately, due to the appearance of inverse powers of the cutoff a in these expressions, these series are not quantitatively useful. The logarithmic dependence in $d=3$ suggests the use of the renormalization group, and this is the subject of the next section.

V. RENORMALIZED PERTURBATION THEORY

As we have discussed, the expressions we have derived for the interface position and width contain terms that become infinite as the cutoff is taken to zero. This is analogous to the situation encountered in trying to compute the Green's function in a quantum-field theory. Often, one can absorb all divergent powers of the cutoff into "renormalized" parameters. If this is the case, physically relevant results will depend only on these parameters

and the theory is said to be "renormalizable." In our case, this would mean that a suitable redefinition of J, v, and g would enable us to take the $a \to 0$ limit. In this section, we will show that this is not the case, at least for $d=3$.

Consider calculating $\langle \tilde{f}_{\mathbf{k}}(s)\eta_{\mathbf{k}}(\xi)\rangle$, where we have defined a transformed variable

$$\tilde{f}_{\mathbf{k}}(s)=\int_0^\infty dt\, e^{-st}\int d\mathbf{x} f(\mathbf{x},t)e^{i\mathbf{k}\cdot\mathbf{x}} .$$

To leading order, the average is given by

$$F^{(1)}\equiv gG_{\mathbf{k}}(s)(2\pi)^{d-1}\left[\frac{\delta(\mathbf{k}+\mathbf{k}')}{s-iv\xi}\right]e^{-a^2(\xi^2+\mathbf{k}^2)}, \tag{24}$$

where we have assumed a Gaussian cutoff on the η correlation which is symmetric in Fourier space, including the longitudinal transform coordinate ξ [in fact, the d-dimensional Fourier transform of (8)]. $G_k(s)$ is the free diffusive propagator $1/(s+Jk^2)$. To order g^3, the five diagrams shown in Fig. 4 contribute. Diagram 4(a) gives rise to the expression

$$F^{3(a)}=G_{\mathbf{k}}(s)\int_0^\infty dt\int_0^t dt'\int_0^{t'} dt''\int d\mathbf{p}\int d\mathbf{q}\, e^{-st}e^{-J\mathbf{p}(t-t')}e^{-J\mathbf{q}^2(t'-t'')}\langle \eta'_{\mathbf{k}-\mathbf{p}}(vt)\eta_{\mathbf{k}'}(\xi)\rangle\langle \eta'_{\mathbf{p}-\mathbf{q}}(vt')\eta_{\mathbf{q}}(vt'')\rangle . \tag{25}$$

After some algebra, this can be rewritten as $i\xi/(s-iv\xi)F^{(1)}I$, with I given by

$$I=\frac{\pi^{(d-2)/2}vg^2}{2a^3}\int_0^\infty d\beta\,\beta(a^2+J\beta)^{-(d-1)/2}e^{-(s-iv\xi)\beta-v^2\beta^2/4a^2} .$$

Specializing to $d=3$, we can perform the integration and keep only the terms divergent in the $a=0$ limit. The result is

$$I=\frac{\sqrt{\pi}v}{2Ja^2}\left[\frac{2\sqrt{\pi}}{v}-\frac{2a(s-iv\xi)}{v^2}+\frac{a}{J}\ln\left[\frac{va}{2J}\right]\right] .$$

The first and third terms on the right-hand side give rise to a velocity renormalization. That is, they can be absorbed to order g^3 by defining

$$v_R=v-\frac{g^2}{Ja}\left[\frac{\pi}{a}+\frac{\sqrt{\pi}v}{J}\right] . \tag{26}$$

Unfortunately, there seems to be no consistent way to absorb the middle term. This piece is subleading in the $t\to\infty$ limit, but we are not sure that it therefore should be discarded.

A similar computation can be carried out for diagrams 4(b). After some work, we can express the sum of the two diagrams in terms of two integrals as

$$F^{3(b)}=G_{\mathbf{k}}(s)F^{(1)}[I_1G_{\mathbf{k}}(s)+I_2] , \tag{27}$$

with

$$I_1=\frac{\sqrt{\pi}}{4a^5}\int_0^\infty d\alpha\frac{1}{a^2+J\alpha}(2a^2-\alpha^2v^2)\exp\left[-\alpha s-a^2k^2-\frac{\alpha^2v^2}{4a^2}\right]\left[\exp\left[\frac{a^4k^2}{a^2+J\alpha}\right]-1\right] ,$$

$$I_2=\frac{-\sqrt{\pi}}{4a^5}\int_0^\infty d\alpha\int_0^\infty d\beta\frac{1}{a^2+J(\alpha+\beta)}[2a^2-(\alpha+\beta)^2v^2]\exp\left[-\frac{v^2(\alpha+\beta)^2}{4a^2}\right]e^{-iv\xi\beta-(\alpha+\beta)s-\alpha Jk^2} .$$

Let us consider I_1 first. If we change variables to $x\equiv v\alpha/2a$, we find that the integral is dominated by $x\sim a$. We can then neglect all the terms in the first exponential in the above expression, and its contribution equals $\pi Jk^2/2a$. Comparing this to the definition of $F^{(1)}$, we can identify a renormalized elastic coefficient

$$J_R=J-\frac{\sqrt{\pi}Jg^2}{2a} . \tag{28}$$

Now consider I_2. It is convenient to change variables to $u=(\alpha+\beta)/2$ and $z=(\alpha-\beta)/a$, which after integrating over z and expanding yields

$$I_2=\frac{\sqrt{\pi}}{4Ja}\int_0^\infty du(2-v^2u^2)\left[\frac{1}{a+Ju}-us-\tfrac{3}{4}u(iv\xi+Jk^2)\right]e^{-v^2u^2/4}$$

$$=\frac{\sqrt{\pi}}{4Ja}\left[\frac{1}{J}\ln\left[\frac{J}{2va}\right]+\frac{1}{v^2}[s+\tfrac{3}{4}(iv\xi+Jk^2)]\right] . \tag{29}$$

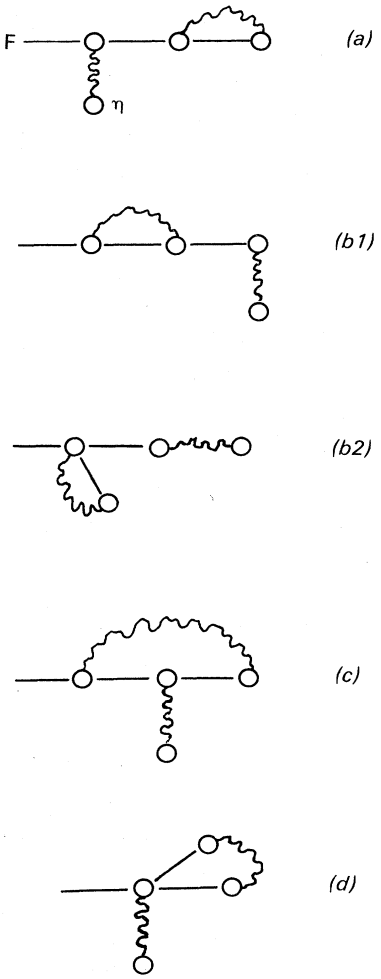

FIG. 4. Diagrams for the fourth-order renormalization calculation.

Again, we do not know how to get rid of these divergences. The first term seems to be a coupling-constant renormalization, in as much as it is independent of k, s, and ξ, but is not consistent with the theory being renormalizable in three dimensions. The second term is similar to the second term above and cannot be absorbed.

Similar computations have been performed for the remainder of the diagrams to this order. There are no wholesale cancellations and hence our theory cannot be made finite perturbatively. There are several reasons for this to have occurred. One possibility is that we have broken rotational invariance by separating out a longitudinal coordinate for special treatment. Indeed, (2) possesses an interface reparametrization invariance which is lost in (3), and in general symmetries are conducive to renormalizability. A related possibility is that we had to include a rescaling of the noise correlation with differing behavior in space and time. These are technical problems that in principle might be resolved. However, we feel that the real reason for the failure of a perturbative approach is the fact that we started with a flat interface, and used the cutoff to smooth out the random-force fluctuations. We expect that the interface can itself generate a finite width and self-consistently average the force on a scale larger than the cutoff. This effect cannot be seen in perturbation theory which, in this sense, always overestimates the effect of the randomness. What we expect to be true is that the prediction via perturbation theory that uniform translation breaks down for $d \leq 3$ is valid for small v, but that the interface may stabilize itself nonperturbatively for large v even in low dimensions. We now turn to numerical simulation of the interface evolution equation to see what actually occurs.

VI. NUMERICAL RESULTS

In the absence of consistent and reliable analytic results we turn to numerical integration of the differential equation (3). Ordinarily the integration of a nonlinear diffusion equation with simple boundary conditions is straightforward,[17] but here the fluctuating random term requires special care. If we discretize on a transverse lattice to give a set of coupled ordinary differential equations of the schematic form $\dot{f}(t)=R(f(t))$, then a variety of stable integration algorithms can be used provided the right-hand side R satisfies the Lipshitz condition $|R(f+\Delta f)-R(f)|<K\Delta f$, for constant K. In the case at hand, a small change in f can cause an $O(1)$ change in η so some smoothing in addition to the latticization is needed. We stick as closely as possible to short-range correlation and take the equations

$$\frac{\partial f(\mathbf{x},t)}{\partial t}=1+J\sum_{i=-(d-1)}^{d-1}[f(\mathbf{x}+\hat{\mathbf{e}}_i,t)-f(\mathbf{x},t)] +gH(\mathbf{x},[f(\mathbf{x},t)]) , \tag{30}$$

$$H(\mathbf{r})=\frac{1}{(2d+1)^{1/2}}\sum_{i=-d}^{d}\eta(\mathbf{r}+\hat{e}_i), \quad \langle\eta(\mathbf{r})\eta(\mathbf{0})\rangle=\delta_{\mathbf{r},0} , \tag{31}$$

where $\mathbf{x}$ is a $(d-1)$-dimensional lattice vector, $[f]$ is the nearest integer to f, $\mathbf{r}=(\mathbf{x},[f])$, and $\hat{\mathbf{e}}_i$ is the unit vector in direction i. Note that we have set the bare velocity $v=1$, by redefining the unit of time and the other couplings J and g in (30). From (31), the correlation function $\langle H(\mathbf{r})H(\mathbf{0})\rangle$ is 1 if $\mathbf{r}=\mathbf{0}$, a constant if $\mathbf{r}$ is a first or second nearest neighbor of $\mathbf{0}$, and 0 otherwise. η is computed by taking the integer part of an algebraic combination of the d components of its argument, and using this integer as the seed for a random number generator. The resulting random numbers are scaled and shifted so as to be uniformly distributed on the interval [-1,1].

Using the nearest-neighbor regularization just described, we have integrated the equations (30) using the general implicit scheme

$$f(t+\Delta t)=f(t)+\Delta t[1+(1-\theta)JD\cdot Df(t) +\theta JD\cdot Df(t+\Delta t)+H] \tag{32}$$

for various values of θ (0, 0.5, and 1.5), as well as a fourth-order Runge-Kutta scheme. If we choose the time

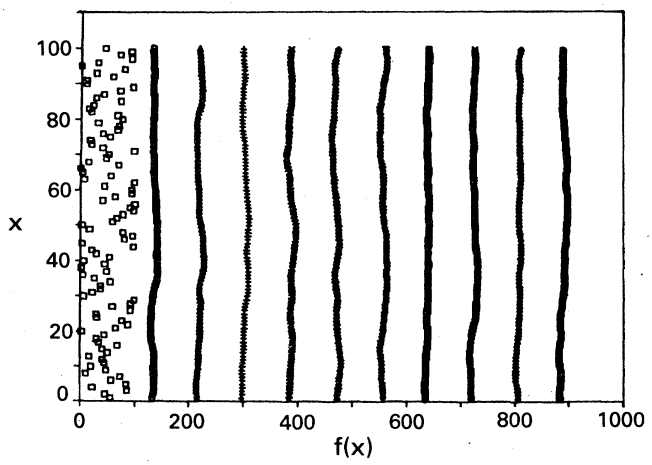

FIG. 5. Snapshots of a 2D interface uniformly translating after a rough start.

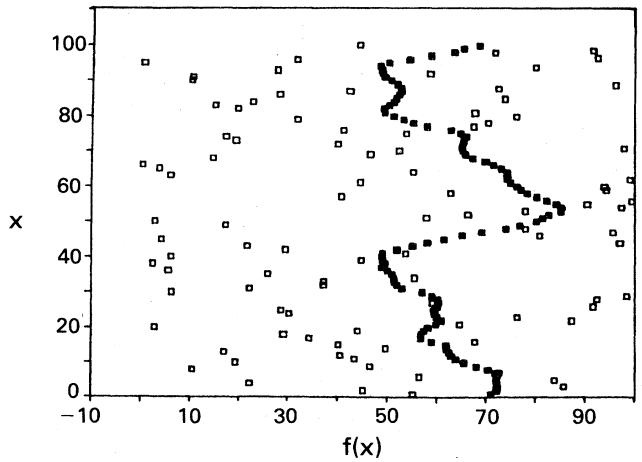

FIG. 7. Pinning of a 2D interface after a rough start.

increment sufficiently small, say $\Delta t \cdot \max [J, gH_{\max}] \lesssim 0.1$, the results are stable with respect to integration method and to further reductions in Δt. In most cases, the bulk of the computation times goes into determining the random function η at different space points.

In Fig. 5, we show a two-dimensional example of the interface for $J=1$ and $g=0.5$, on a 100-site lattice periodic in the transverse direction. The starting interface is "rough," with random initial values, and its evolution is shown at intervals of 100 time units. We see that in this regime the interface is more or less planar and translating with constant velocity. If the random strength g is increased to 1.5, the interface becomes pinned. In Fig. 6, we show $f(x)$ at $t=0$, 100, and 200 when the initial shape is the plane $f=0$, and in Fig. 7 the same thing for a rough initial interface. At later times the interface is fixed, except for an occasional jiggle. The subsequent results refer to the average behavior of the interface as a function of J, g, and the spatial dimension d, defined as ensemble averages over the random function η. We simulate different elements of the ensemble by choosing planar initial interfaces located at different longitudinal coordinates. In most cases we average over five realizations, finding statistical errors of at worst 10% in such quantities as the average velocity and critical pinning strength.

In two dimensions (2D), we find that the interface becomes pinned once the random strength g exceeds a critical value $g_c(N,J)$. The variation of g_c with transverse size N is shown in Fig. 8; pinning is easier on a small lattice, as fewer constraints need be satisfied, but for $N > O(100)$ the critical value saturates at about 1.2. The scaling result (14) implies that $g_c \sim J^{1/4}$, but the numerical results shown in Fig. 9 for g_c as a function of J at $N=100$ show a variation that is no stronger than logarithmic over a four decade range. The behavior of the interface as the pinning transition is approached is illustrated in Fig. 10, where we plot the average velocity as a function of g at $J=1$ and two different values of N. Below the transition, $\langle v \rangle$ decreases smoothly from 1 as g increases from 0, along what appears to be a universal curve, but then drops abruptly near $g_c(N)$. The next set of figures show the interface (rms) width as a function of the parameters. In Fig. 11 we see that the width in the pinned phase is a roughly logarithmic function of the transverse size, also in contradiction to the scaling argument of Ref. 9, which predicts power dependence. Figure 12 gives w as a function of g for $N=100$ and $J=1$ as g_c is approached from below, and Fig. 13 shown that w also

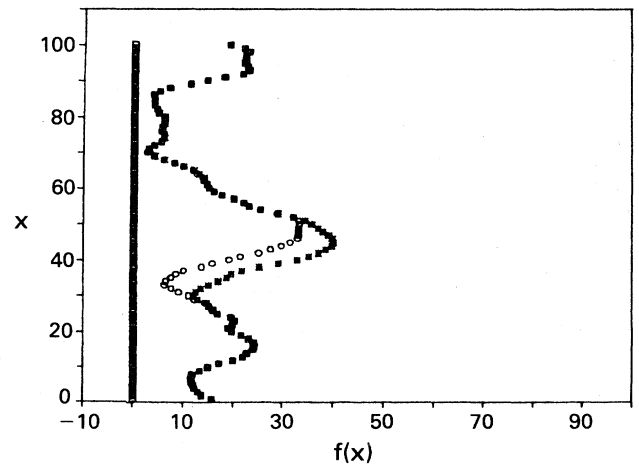

FIG. 6. Pinning of a 2D interface after a planar start.

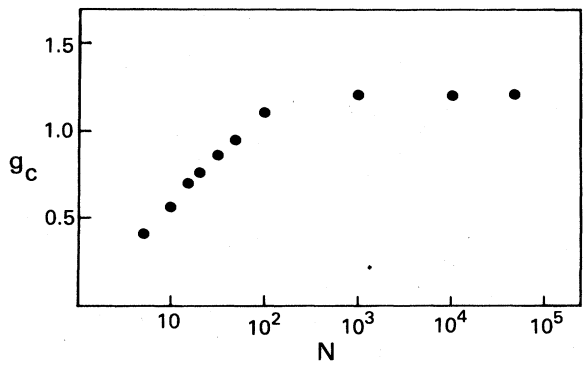

FIG. 8. Variation of critical pinning strength g_c with transverse N size in 2D.

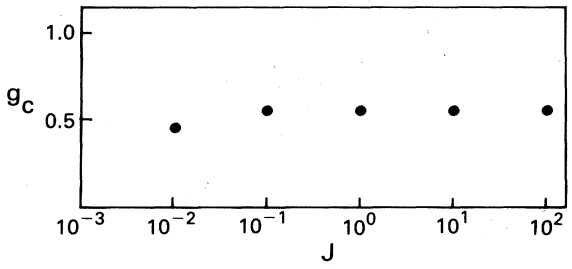

FIG. 9. Variation of g_c with elastic coupling J in 2D.

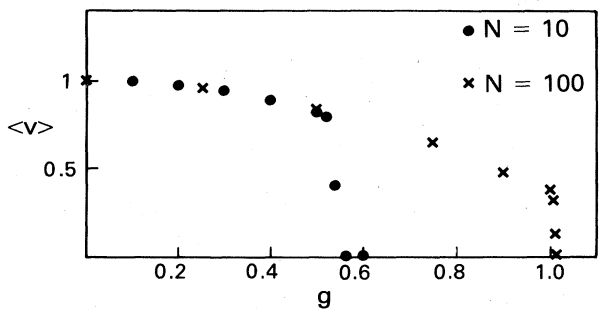

FIG. 10. Variation of average velocity with g in 2D.

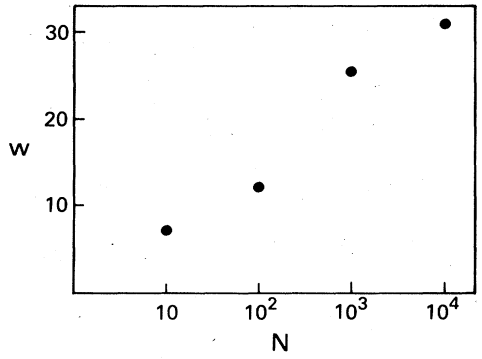

FIG. 11. Variation of interface width w with N in 2D.

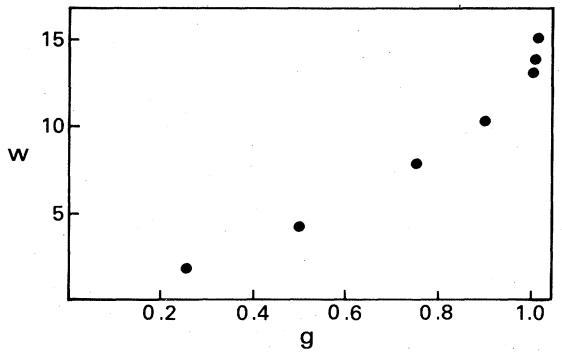

FIG. 12. Variation of w as $g \rightarrow g_c -$ in 2D.

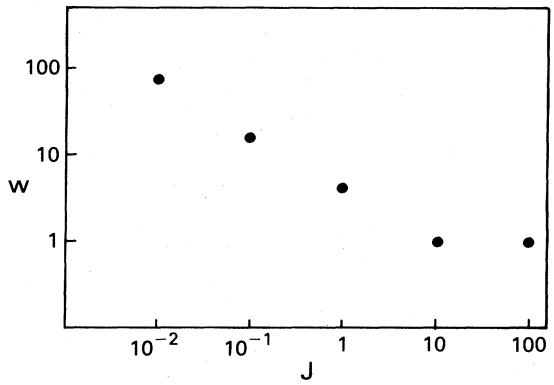

FIG. 13. Variation of w with J in 2D.

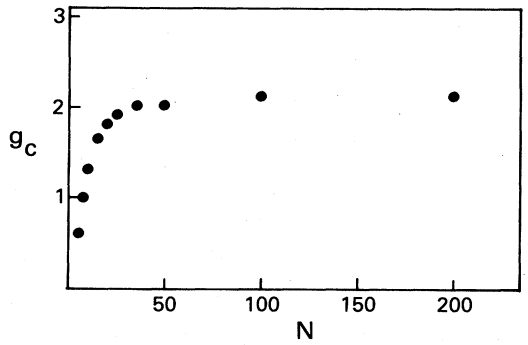

FIG. 14. Variation of g_c with N in 3D.

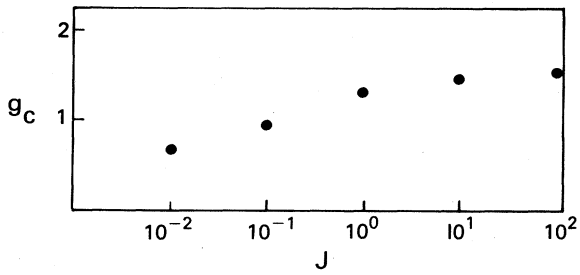

FIG. 15. Variation of g_c with J in 3D.

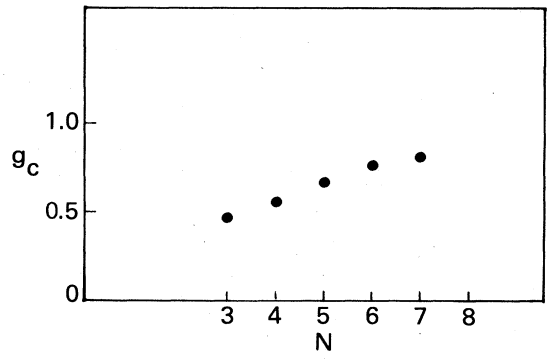

FIG. 16. Variation of g_c with N in 4D.

varies logarithmically with J for $N=100$ in the moving regime, again not the prediction of the scaling argument.

In three dimensions, the behavior is qualitatively the same. Figure 14 shows the variation of g_c with (linear) transverse size N, and again there is an increase at small values of N which saturates for $N > O(100)$. Figure 15 gives g_c versus J, again logarithmic rather than the $J^{1/2}$ dependence predicted by scaling. The other curves displayed for the 2D case have more or less the same form in 3D.

In four dimensions the behavior changes. For small lattices, $N \leq 7$, there is a pinning transition at finite g, as shown in Fig. 16, with g_c again an increasing function of N. However, for $N > 7$ pinning does not occur for any g. This is most conveniently illustrated by showing the variation of average velocity with g; Fig. 17(a) shows $\langle v \rangle$ tending monotonically to zero as g increases for $N=6$ and 7, but for $N=8$ and 9 we see in Fig. 17(b) that increasing randomness does not suffice to pin the interface. In $d \geq 4$ the width is never larger than a few lattice units, and this suffices to apply the argument given around Eq. (11). In still higher dimensions, we presume the behavior will be the same, but the numerical computations become very time consuming and we have not checked this explicitly.

We conclude with a remark on the importance of interface overlap, a possibility not taken account of in a solid-on-solid model. In dimension four (and presumably above) where pinning is absent, the interface tends to be quite flat and overlaps are simply irrelevant. In lower dimensions where the pinning occurs, this is no longer true. One might expect the possibility of overlap to enhance the likelihood of pinning, on the grounds that transverse motion is now possible and there is more opportunity to find a configuration of local equilibrium. Thus, the critical pinning dimensions should not be affected, although the detailed behavior of pinned configurations may differ.

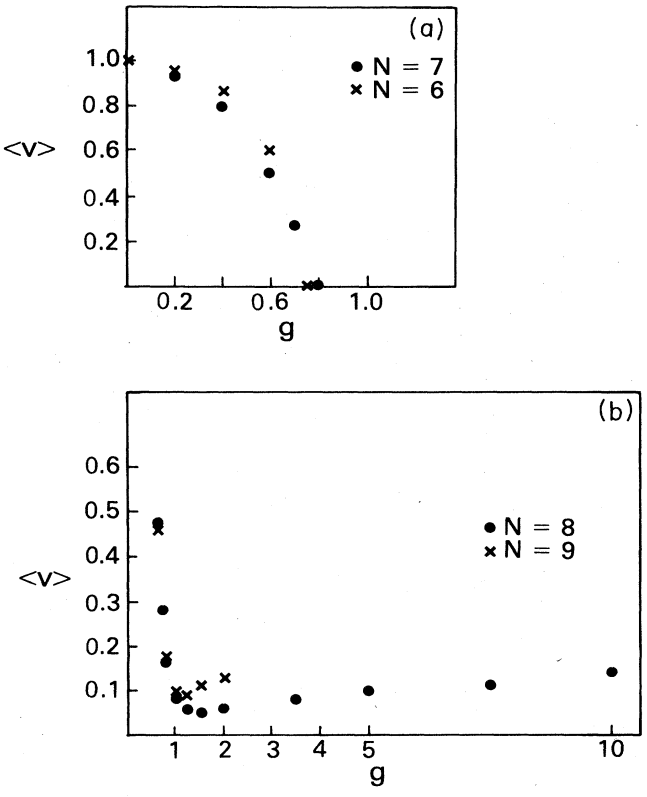

FIG. 17. Average velocity vs g in 4D, (a) $N=6$ and 7 where pinning occurs, and (b) $N=7$ and 8 where it does not.

VII. CONCLUSIONS

We have introduced and discussed the properties of a model stochastic differential equation which describes the motion of a phase domain or interface driven through a random background medium. We and others[9] have presented a variety of analytic arguments which are not all mutually consistent and which are somewhat inconclusive, and have attempted to resolve the situation by numerical integration. The model has pinned solutions for sufficiently large randomness in dimensions $d \leq 3$, while for weak randomness in $d \leq 3$ and any randomness in higher d the solution is a nearly planar interface propagating with constant velocity. The numerical results are consistent with mean-field theory in the sense that both pinned and translating solutions exist there, and consistent with perturbation calculations to the extent that the latter only allows uniformly translating solutions for $d > 3$, but they disagree with the scaling arguments of Ref. 9. We have attempted to use a variety of other analytic techniques, including the Liouville equation,[5] iterative solutions of the schematic form

$$f_{n+1} = vt + \int G\eta(f_n) ,$$

and the Martin-Siggia-Rose[18] formalism, none of which has been productive. It is our feeling that the model equation (3) is an obvious simple description of an interface in a random background, and reliable analytic results would be most desirable.

The implications of this model for fluid displacement in porous media are as follows. The existence of a pinning regime at (in effect) low external driving force corresponds nicely to the phenomenon of invasion percolation[8] at low flow rates, where the macroscopic average interface does not move. The model predicts that in spatial dimension $d \geq 4$ the interface will instead always propagate as a plane, which means that the extraction of oil from high-dimensional hydrocarbon reservoirs should be very efficient. The qualitative features of the interface in the moving regime are also reproduced. Planar propagation with a relatively narrow width is observed when the displacing fluid is more mobile than that displaced. As mentioned at the outset, this is what corresponds to our choice of the local evolution equation. In the case of the displacing fluid being less mobile, the interface is observed to be unstable and "fingered" on the macroscopic scale.[3] The latter case could perhaps be modeled by choosing $J<0$ and adding a positive $\nabla^4 f$ term for stability, in analogy with our work on the related macroscopic instability in dendritic crystal growth, but we have not pursued this idea any further.

With regard to random Ising systems, we are in qualitative agreement with the discussions of Bruinsma and Aeppli[9] and Villain.[11] In dimensions accessible to experiment (two or three), we support their prediction of pinned interfaces and concomitant metastable states at large randomness. (Villain, and also Grinstein and Fernandez,[19] have gone on to argue that the decay of such metastable domains will be logarithmic in time, by estimating the effects of thermal fluctuations.) Some of the specific quantitative scaling predictions, such as (14) for the depinning strength, do not, however, agree with our numerical calculations. In the absence of reliable analytic results we are unable to make more precise statements about the magnetic experiments.

ACKNOWLEDGMENT

We thank R. Bruinsma for a discussion of Ref. 9 and R. Dashen, M. Muthukumar, and A. Zee for their collaboration at various stages of this work.

[1]Proceedings of the Los Alamos Conference on Fronts, Interfaces and Patterns [Physica **12D**, 1 (1984)].

[2]R. C. Brower, D. Kessler, J. Koplik, and H. Levine, Phys. Rev. Lett. **51**, 1111 (1983); Phys. Rev. A **29**, 1335 (1984); D. Kessler, J. Koplik, and H. Levine, *ibid.* **30**, 3161 (1984); **31**, 1712 (1985); E. Ben-Jacob, N. Goldenfeld, J. S. Langer, and G. Schön, Phys. Rev. Lett. **51**, 1930 (1983); Phys. Rev. A **29**, 330 (1984); E. Ben-Jacob, N. Goldenfeld, G. Kotliar, and J. S. Langer, Phys. Rev. Lett. **53**, 2110 (1984).

[3]See, for example, A. E. Scheidegger, *The Physics of Flow in Porous Media,* 3rd ed. (University of Toronto Press, Toronto, 1984); J. Bear, *Dynamics of Fluids in Porous Media* (Elsevier, New York, 1972).

[4]J. Koplik and T. J. Lasseter, Chem. Eng. Commun. **26**, 285 (1984); Soc. Pet. Eng. J. **25**, 89 (1985); M. M. Dias and A. C. Payatakes (unpublished).

[5]N. G. van Kampen, *Stochastic Processes in Physics and Chemistry* (North-Holland, Amsterdam, 1981).

[6]J. D. Weeks, in *Ordering in Strongly Fluctuating Condensed Matter Systems,* edited by T. Riste (Plenum, New York, 1980); M. Wortis, in *Ordering in Two Dimensions,* edited by S. Sinha (North-Holland, Amsterdam, 1980).

[7]R. Chandler, J. Koplik, K. Lerman, and J. F. Willemsen, J. Fluid Mech. **119**, 249 (1982); D. Wilkinson and J. F. Willemsen, J. Phys. A **16**, 3365 (1983); R. Lenormand and S. Bories, C. R. Acad. Sci. Paris B **291**, 279 (1980); R. Lenormand and C. Zarcone, Phys. Rev. Lett. **54**, 2226 (1985).

[8]A. C. Payatakes, Annu. Rev. Fluid Mech. **14**, 365 (1982).

[9]R. Bruinsma and G. Aeppli, Phys. Rev. Lett. **52**, 1547 (1984).

[10]G. Grinstein and S.-k. Ma, Phys. Rev. B **28**, 2588 (1983); for a review, see G. Grinstein, J. Appl. Phys. **55**, 2371 (1984).

[11]J. Villain, Phys. Rev. Lett. **52**, 1543 (1984).

[12]K. Kawasaki and T. Ohta, Prog. Theor. Phys. **67**, 147 (1984).

[13]E. Marinari, G. Parisi, D. Ruelle, and P. Windey, Phys. Rev. Lett. **50**, 1223 (1983); M. Luck, Nucl. Phys. **225B**, 169 (1983); D. S. Fisher, Phys. Rev. A **30**, 960 (1984).

[14]M. Eden, in *Proceedings of the Fourth Berkeley Symposium on Probability and Statistics,* edited by J. Neyman (University of California Press, Berkeley, 1961), Vol. 4, p. 223.

[15]T. A. Witten and L. M. Sander, Phys. Rev. B **27**, 5686 (1983).

[16]A similar mean-field argument has been given by D. S. Fisher, Phys. Rev. Lett. **50**, 1486 (1983), and unpublished.

[17]See, e.g., E. Isaacson and H. B. Keller, *Analysis of Numerical Methods* (Wiley, New York, 1966).

[18]P. C. Martin, E. D. Siggia, and H. A. Rose, Phys. Rev. A **8**, 423 (1973).

[19]G. Grinstein and J. F. Fernandez, Phys. Rev. B **29**, 6389 (1984).